Population inversion in sodium D_2 transition based on sodium-ethane excimer pairs

Shu Hu (胡 墅)[1], Baodong Gai (盖宝栋)[1,2], Jingwei Guo (郭敬为)[1,*], Pengyuan Wang (王鹏远)[1], Xueyang Li (李学杨)[1,2], Hui Li (李 慧)[1], Jinbo Liu (刘金波)[1], Shan He (何 山)[1,2], Xianglong Cai (蔡向龙)[1], Dong Liu (刘 栋)[1], Ying Chen (陈 莹)[1], Fengting Sang (桑凤亭)[1], and Yuqi Jin (金玉奇)[1]

[1]*Key Laboratory of Chemical Lasers, Dalian Institute of Chemical Physics, Chinese Academy of Sciences, Dalian 116023, China*

[2]*University of Chinese Academy of Sciences, Beijing 100049, China*

**Corresponding author: jingweiguo@dicp.ac.cn*

Received July 10, 2017; accepted July 28, 2017; posted online August 21, 2017

Sodium-ethane excimer pairs are studied and proved to be a great choice of excimer pumped sodium laser (XPNaL) gain media. The lifetime of the sodium D_2 line is studied in a sodium-ethane excimer system excited by a 553 nm laser, and the observed phenomenon of lifetime lengthening is discussed. Amplified spontaneous emission (ASE) of the sodium D_2 line is successfully obtained, and its time-resolved and spectroscopic characteristics are studied experimentally. According to the intensity of the ASE signal under different sodium vapor atom densities, the sodium D_2 line gain feature of sodium-ethane excimer pairs excited by the 553 nm laser is concluded.

OCIS codes: 140.1340, 140.2180, 020.0020.

doi: 10.3788/COL201715.111401.

In recent years, the diode pumped alkali laser (DPAL) has attracted extensive attention and study in the field of high power laser due to its advantages, such as high gain coefficient, small medium volume, high quantum efficiency, good beam quality, and excellent flowing and heat dissipation properties[1,2]. DPALs based on potassium[3], rubidium[4], and cesium[5] vapors have achieved great progress recently. The excimer pumped alkali laser (XPAL)[6,7] is a new class of optically pumped laser, which is developed from the DPAL. Thanks to the excimer pairs, XPAL can realize broad absorption; this feature avoids the problem of linewidth matching between the absorption of alkali metal vapor and the emission of diode laser. XPAL based on Cs vapor has been reported of lasing on the D_1 line (894 nm)[8] and D_2 line (852 nm)[9]. The D_2 line (780 nm) of Rb vapor laser has also been demonstrated experimentally[10]. Furthermore, the blue light can be realized in Rb vapor based on frequency upconversion[11].

For the splitting between energy levels of $3^2P_{3/2}$ and $3^2P_{1/2}$ of just 17.2 cm^{-1}[1], it will be difficult to realize a DPAL operating as a three-level system based on sodium vapor. Fortunately, XPAL is a four-level or five-level system, which can avoid the energy level splitting problem mentioned above, and can make lasing of sodium vapor possible. The sodium D_1/D_2 line laser from the excimer pumped sodium laser (XPNaL) will be suitable for the application of the sodium beacon laser, which is the light source of the sodium guide star. The sodium guide star can improve the image resolution of the adaptive optics (AO) system[12,13] at high altitudes and is essential for applications such as universe observation, space target recognition, and laser telecommunications[14,15]. The prevalent sodium beacon lasers are mainly based on methods of sum-frequency generation (SFG)[16] of 1064 and 1319 nm[17], stimulated Raman scattering (SRS)[18], and an optical parametric amplifier (OPA)[19]. If XPNaL is utilized as a sodium beacon laser, a wavelength correction system is unnecessary. Sodium-ethane excimer pairs will be formed after the collision happens between sodium atoms of the ground state ($3^2S_{1/2}$) and ethane molecules, and a "blue satellite" pumping laser will excite excimer pairs from the $X^2\Sigma^+_{1/2}$ state to the $B^2\Sigma^+_{1/2}$ state. Since the $B^2\Sigma^+_{1/2}$ is a repulsive state, excimer pairs dissociate quickly to produce sodium atoms of an excited state ($3^2P_{3/2}$), then the sodium D_2 line laser can be observed from the stimulated emission of $3^2P_{3/2} \rightarrow 3^2S_{1/2}$ and accurately match the resonance line of the sodium atom, so XPNaL provides a novel technical approach for the sodium beacon laser.

In 2012, Hewitt and Eden realized XPNaL based on Na–Xe excimer pairs lasing at sodium D_1 and D_2 lines[20], however, suffering from the low pumping efficiency, the laser power was too low. So, the key issue of developing XPNaL is exploring excellent excimer pairs. In our previous work, we expanded the sodium-rare gas pairs to sodium-alkane gas pairs, and studied the absorption coefficients of different excimer pairs, including Na-C_2H_6 excimer pairs, both experimentally and theoretically[21].

In this work, the fluorescence lifetime of the sodium D_2 line based on Na-C_2H_6 excimer pairs is measured, and the kinetic process of fluorescence lifetime lengthening is given. The time-resolved and spectroscopic characteristics of the sodium D_2 line amplified spontaneous emission (ASE), also the sodium D_2 line gain feature of Na-C_2H_6 excimer pairs, is investigated through the ASE intensity

testing under different sodium vapor atom density. The Na-C_2H_6 system is considered to own the potential to be utilized in high power XPNaL.

The experiment scheme of XPNaL D_2 line fluorescence lifetime and ASE is shown in Fig. 1, the second harmonic of an Nd:YAG (PRO-290-30EH, Spectral Physics) with 30 Hz repetition frequency is utilized to pump a dye laser (Narrow ScanK, Radiant Dyes), where the wavelength tuning range of the dye laser is from 545 to 570 nm, and the pulse duration is around 8 ns (full width at half-maximum, FWHM). The dye laser was tuned to 553 nm in *p*-polarization to excite Na-C_2H_6 excimer pairs.

The sodium vapor cell is manufactured using borosilicate glass with a length of 10 cm and a diameter of 2.5 cm. Plenty of sodium metal is introduced into the cell, and ethane with a pressure of 600 torr (at 25°C) is filled in the cell as a buffer gas. The operation temperature of the cell is accurately controlled by an oven with a temperature controller. An optical fiber is used to couple the light signal into a spectrometer (JY FHR1000), then, the synchronization between the Nd:YAG laser and the ICCD detector of the spectrometer used is realized by a time delay generator (DG645, Stanford Research System).

Time-resolved fluorescence spectroscopy is realized by the experimental equipment mentioned above. For the fluorescence lifetime measurement of the sodium D_2 line, the fiber end is placed facing the small window on the center of one side surface of the oven, and after setting the trigger time and exposure time of ICCD, the fluorescence intensity will be recorded on the ICCD by time slicing processing. When measuring the sodium D_2 line ASE signal, a polarizing beam splitter (PBS) is used to isolate the ASE signal in *s*-polarization from the transmission pumping laser in *p*-polarization, a grating is used to completely separate the ASE signal from the residual pumping laser in *s*-polarization, and, with that, the detection sensitivity of ICCD can be ensured.

We have tried using the time-resolved fluorescence spectroscopy to measure the pulse shape of the dye laser, and the measured error is about 0.2 ns. However, the fluorescence lifetime of the sodium D_2 line is around dozens of nanoseconds, so the measurement accuracy of this time-resolved fluorescence spectroscopy can be accepted.

The sodium vapor cell is heated to 300°C; before measuring the fluorescence lifetime, the exposure time of the ICCD is set to 500 ns, and after excitation of 553 nm pumping laser, the fluorescence signals of the sodium D_1 and D_2 lines are acquired as the inset of Fig. 2. These two lines are separated, and they own almost equal intensities; the equal intensities are thought to be a result of the sufficiently rapid mixing rate of the fine structure due to the small energy level splitting (17.2 cm^{-1}) between the $3^2P_{3/2}$ and $3^2P_{1/2}$ states.

Then, the exposure time of the ICCD is set to 6 ns, and the fluorescence spectrum is recorded under different trigger times, successively. The fluorescence intensity decaying accords with the exponential decaying, and it has the expression

$$y = Ae^{-t/\tau}, \tag{1}$$

where y is intensity of the fluorescence signal, A is a constant, and τ is the fluorescence lifetime. In order to reduce the fitting error, the natural logarithm of fluorescence intensity is used here, the Eq. (1) can be rewritten as

$$\ln y = -t/\tau + \ln A. \tag{2}$$

The intensity of the fluorescence signal decay based on Eq. (2) is depicted in Fig. 2. We ignore the earliest few data points in the pumping duration, and the last few data points with bad linearity, and after linear fitting of the middle data, we obtain that the sodium D_2 line fluorescence lifetime of Na-C_2H_6 excimer pairs is 33.3 ns with an error bar of 0.4 ns. The natural fluorescence lifetime of the sodium D_2 line is reported to be 16.254 ns[22], however, as the buffer gas filled in the cell, the measured lifetime after the dissociation of Na-C_2H_6 excimer pairs is obviously longer than 16.254 ns. The pits of the sodium D_1 and D_2 lines (the inset spectrum of Fig. 2) are caused by the reabsorption of sodium atoms in the unpumped region. Also, this demonstrated that stark broadening occurred on fluorescence lines[23,24], because the broadening is so wide. The reabsorption could not influence the measured lifetime fitted on fluorescence intensity. Except for the sodium D_2 line, the measured lifetime of the sodium D_1

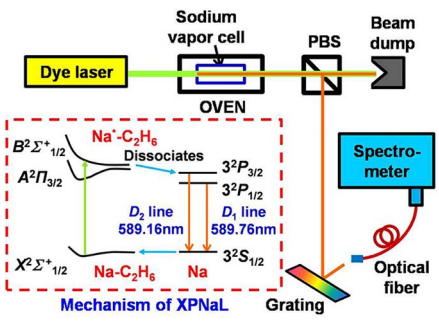

Fig. 1. Experiment scheme of XPNaL fluorescence lifetime and ASE.

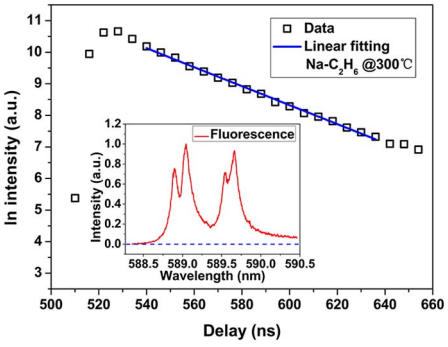

Fig. 2. Fluorescence decaying of Na D_2 line. Inset: a spectrum of sodium fluorescence.

line also is lengthened as 32.8 ns with an error bar of 0.4 ns. We believed that the radiation trapping effect lengthened the measured lifetime of the sodium D_1 and D_2 lines; similar phenomena had been reported that as atom density is increased, the obtained lifetimes of the $3^2P_{3/2}$ and $3^2P_{1/2}$ states are lengthened obviously after being excited by resonance radiation[25,26]. Fluorescence spectra of the sodium D_1 and D_2 lines are asymmetric, respectively, especially the continuous spectrum beside the sodium D_1 line. This is caused by excimer transition, and the measured lifetime of the continuous spectrum is 32.8 ns with an error bar of 0.5 ns, which is basically the same with the sodium D_1 and D_2 lines.

The radiation trapping effect is a common physical phenomenon in alkali vapor, moreover, the quenching effect will occur simultaneously due to the buffer gas used in the alkali vapor laser[27,28]. As the operation temperature is raised, the measured lifetime will be lengthened further, owning to the enhancing of the radiation trapping effect by the increasing alkali vapor atom density. Meanwhile, more time is available for quenching to take place. When increasing the pressure of buffer gas to suppress the effect of radiation trapping, the quenching effect will become larger due to the increasing buffer gas molecules' density[29]. Methane and ethane are excellent buffer gases with small quenching cross-sections, so these molecules will not cause significant $n^2P \rightarrow n^2S$ quenching[29,30]. Owning to the small quenching effect on the sodium $3^2P_{3/2}$ state of Na-C_2H_6 excimer pairs, the population inversion and the threshold of lasing will not be obviously impacted.

The time-resolved and spectrum characteristic of the sodium D_2 line ASE signal are studied experimentally. The operation temperature of the sodium vapor cell is increased to 310°C. After Na-C_2H_6 excimer pairs are excited by the 553 nm pumping laser, the detected signal from the end window is depicted in Fig. 3(Inset), and in comparison with the fluorescence signal in Fig. 2, the linewidth of the detected signal is much narrower. The linewidth value is less than 0.02 nm (FWHM), and it accords with the narrow linewidth characteristic of the ASE signal. A sodium D_2 ASE means that the sodium D_2 line fluorescence signal is amplified rapidly along the direction of the pumping laser by the population inversion between the $3^2P_{3/2}$ state and ground state. By changing the pumping pulse energy, the sodium D_2 line ASE intensity growth is shown in Fig. 3, and a linear relationship is observed. The threshold for the sodium D_2 ASE is ~3.5 mJ of pump pulse energy. If the pump energy is less than the threshold, fluorescence signals of the sodium D_1 and D_2 lines will be just measured.

By accurately controlling the trigger and exposure time of the ICCD, the time-resolved characteristic of the sodium D_2 line ASE signal was investigated. We found the pulse shape waveform of the dye laser and the sodium D_2 line ASE signal's own Gaussian distribution profile, just as depicted in Fig. 4. The pulse duration of the ASE signal is 4.3 ns (FWHM), which is obviously shorter than that of dye laser (8.7 ns, FWHM). A lasing process and an ASE process are similar since they both require population inversion. They are similar in many characteristics. So, the time-resolved characteristic of the sodium D_2 line ASE can be alternatively used to estimate and evaluate a possible sodium D_2 line laser.

Small signal gain is usually utilized to evaluate the amplification characteristic of a laser system. The traditional method of small signal gain is based on the variation of a small signal after it passes through the gain media with a certain length, and the gain could be given by the expression

$$g = (1/L) \cdot \ln(I/I_s), \tag{3}$$

where g is the small signal gain, L is the length of gain media, I_s is the intensity of input small signal, and I is the intensity of the output amplified signal. However, it is difficult to measure the D_1 or D_2 line small signal gain of the XPAL by this method. The lower laser level of the XPNaL is the sodium ground state with a population existing throughout. When the gas medium is excited, the strong absorption of sodium D_1 or D_2 lines can overwhelm the small gain. When there is an ASE signal generated by strong excitation, the small signal gain can be interfered and cannot be differentiated. On the other hand, the ASE is an optical amplification process, so we can evaluate the amplification characteristic of the

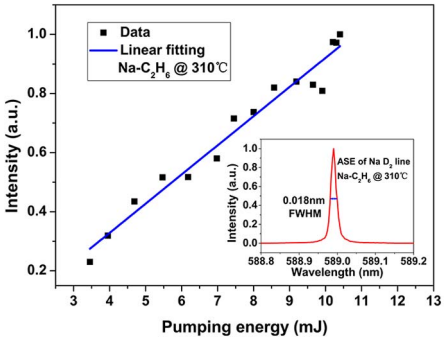

Fig. 3. Intensity increasing of the sodium D_2 line ASE signal with the pumping pulse energy. Inset: the sodium D_2 line ASE spectrum.

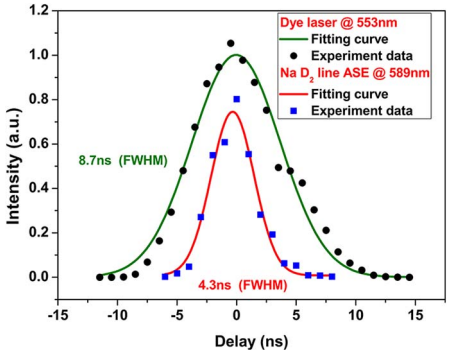

Fig. 4. (Color online) Waveform comparison between the sodium D_2 line ASE and pumping laser.

Na-C_2H_6 excimer pairs by the sodium D_2 line ASE signal under different atom densities of different operation temperatures. Referring to Eq. (3), we use the stimulated emission coefficient to evaluate the sodium D_2 line gain feature, just as the expression in

$$I_{\mathrm{ASE}} = I_0 \exp([\mathrm{Na}] \cdot G_{\mathrm{ASE}} \cdot L), \tag{4}$$

where I_{ASE} is the intensity of the ASE signal, I_0 is the intensity of the initial spontaneous emission signal, [Na] is the sodium vapor atom density (cm^{-3}) without the density of Na-C_2H_6 excimer, G_{ASE} is the sodium D_2 line stimulated emission coefficient (cm^2), which is in the form of macroscopic and average value, and L is the length of the vapor cell (cm). The gain of the sodium D_2 line is provided by sodium atoms, so when calculating [Na], the excimer density should be excluded. Before the pumping laser excites the gain medium, the sodium vapor atom density of the $3^2S_{1/2}$ state and excimer density of the $X^2\Sigma^+_{1/2}$ state can be calculated. Under the condition of thermal equilibrium, the ratio between the population densities on the $X^2\Sigma^+_{1/2}$ state and the $3^2S_{1/2}$ state is decided by the equilibrium fraction, just as is shown in[31]

$$f_{10} = \frac{n_1}{n_0} = \frac{g_1}{g_0} 4\pi R_0^2 \Delta R \exp\left(\frac{-\Delta E_{10}}{k_b T}\right)[\mathrm{C_2H_6}], \tag{5}$$

where f_{10} is the equilibrium fraction, n_0 and n_1 are the population densities on the $3^2S_{1/2}$ state and the $X^2\Sigma^+_{1/2}$ state, respectively, g_0 or g_1 is the degeneracy factor of the $3^2S_{1/2}$ state (2) or the $X^2\Sigma^+_{1/2}$ state (2), R_0 is the optimal internuclear separation (0.4518 nm for Na-C_2H_6)[21], ΔR is the range of distances over which the resonance absorption condition is maintained (0.1 nm)[31], k_b is the Boltzmann constant, T is the temperature of the vapor cell, ΔE_{10} is the difference in the potential energy between the collision pair state at R_0 and the unbound state ($\sim$114.4 cm^{-1})[21], and [C_2H_6] is the ethane concentration (1.94×10^{-19} cm^3).

The sum of the Na containing species must obey conservation, $n_0 + n_1 = n_{\mathrm{Na}}$, and n_{Na} will be calculated indirectly by saturated vapor pressure $P_{\mathrm{Na}}(\mathrm{Pa}) = 10^{9.71-5377/T}$ at different temperatures[32]. The results indicated that the population density of the excimer is lower than that of the sodium atom in two orders of magnitude. Then, we measured the intensity of the sodium D_2 line ASE signal from 330°C to 370°C under the saturation pumping condition and processed the intensity variation curve by exponential fitting, as shown in Fig. 5. It is observed that the experimental data is well consistent with the fitting curve, and G_{ASE} is obtained as $(5.4 \pm 0.5) \times 10^{-17}$ cm^2 after fitting under the pump intensity of 17.7 $\mathrm{MW/cm}^2$. It should be noticed that G_{ASE} is different from the stimulated emission cross-section σ_{30} between the $3^2P_{3/2}$ and $3^2S_{1/2}$ states[20]. G_{ASE} could characterize the property of the gain. G_{ASE} only gives a relative value; it is associated with the intensity of the pump laser.

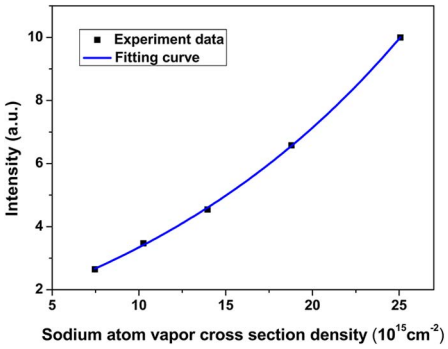

Fig. 5. Sodium D_2 line ASE intensity versus sodium atom vapor density.

As the sodium vapor atom density improved, the sodium D_2 line intensity increased rapidly with an exponential form. So this result demonstrates that the Na-C_2H_6 excimer pairs own good amplification characteristics. Excimer pairs transit sodium atoms from the $3^2S_{1/2}$ state to the $3^2P_{3/2}$ state, just as that described in the mechanism of the XPNaL. Then, the processes of population inversion and amplification will only have a relationship with sodium atom populations at ground and excited states. Since the gain of the alkali atom is high, the good amplification characteristic here can be explained.

At present, all of the reported XPALs generate very weak laser power because they suffer the low level of population inversion limited by the low probability of excimer pairs formation and weak absorption of the pumping laser. By selecting excellent excimer pairs, the probability and absorption mentioned above will be improved, and Na-C_2H_6 excimer pairs can be expected to be a good choice for XPNaL. It is hoped that metal materials (stainless steel or oxygen-free copper) and sapphire windows instead of borosilicate glass can be used in the future. This will increase the lifetime of cells and decrease the negative effects about sodium vapor corrosion and ethane carbonization.

By using the time-resolved fluorescence spectrometer, the sodium D_2 line fluorescence lifetime of Na-C_2H_6 excimer pairs is measured with the value of 33.3 ± 0.4 ns. The lengthened lifetime is explained with radiation trapping. The spectrum and time-resolved characteristics of the sodium D_2 line ASE signal are studied experimentally and can be alternatively used for studying laser signals in the future. Moreover, by measuring the ASE signal intensity under different sodium vapor atom densities, the sodium D_2 line amplification characteristic of the Na-C_2H_6 excimer pairs is studied, and the stimulated emission coefficient G_{ASE} of the sodium D_2 line is obtained as $(5.4 \pm 0.5) \times 10^{-17}$ cm^2 (under the pump intensity of 17.7 $\mathrm{MW/cm}^2$) experimentally. If employing the Na-C_2H_6 excimer pairs for the XPNaL, population inversion between the $3^2P_{3/2}$ and $3^2S_{1/2}$ states can be ensured. By utilizing similar techniques, as used in flowing DPAL, the heat dissipation and ethane carbonization problems

will be solved. Then, Na-C_2H_6 excimer pairs will have the potential for the application of high power XPNaL.

This work was supported by the National Natural Science Foundation of China under Grant Nos. 61505210 and 11475177.

References

1. W. F. Krupke, Prog. Quantum Electron. **36**, 4 (2012).
2. R. H. Page, R. J. Beach, and V. K. Kanz, Opt. Lett. **31**, 353 (2006).
3. B. V. Zhdanov, M. D. Rotondaro, M. K. Shaffer, and R. J. Knize, Opt. Commun. **354**, 256 (2015).
4. J. Zweiback and W. F. Krupke, Opt. Express **18**, 1444 (2010).
5. B. V. Zhdanov, G. Venus, V. Smirnov, L. Glebov, and R. J. Knize, Rev. Sci. Instrum. **86**, 083104 (2015).
6. J. D. Readle, *Atomatic Alkali Lasers Pumped by the Dissociation of Photoexcited Alkali-rare Gas Collision Pairs* (University of Illinois, 2010).
7. A. D. Palla, D. L. Carroll, J. T. Verdeyen, and M. C. Heaven, J. Phys. B: At. Mol. Opt. Phys. **44**, 135402 (2011).
8. J. D. Readle, J. T. Verdeyen, J. G. Eden, S. J. Davis, K. L. Galbally-Kinney, W. T. Rawlins, and W. J. Kessler, Opt. Lett. **34**, 3638 (2009).
9. J. D. Hewitt, T. J. Houlahan Jr, J. E. Gallagher, D. L. Carroll, A. D. Palla, J. T. Verdeyen, G. P. Perram, and J. G. Eden, Appl. Phys. Lett. **102**, 111104 (2013).
10. D. Yue, W. Li, H. Wang, Z. Yang, and X. Xu, Proc. SPIE **8551**, 855102 (2012).
11. R. Cao, B. Gai, J. Yang, T. Liu, J. Liu, S. Hu, J. Guo, Y. Tan, S. He, W. Liu, H. Cai, and X. Zhang, Chin. Opt. Lett. **13**, 121903 (2015).
12. W. Liu, L. Dong, P. Yang, and B. Xu, Chin. Opt. Lett. **14**, 020101 (2016).
13. B. Dong and R. Wang, Chin. Opt. Lett. **14**, 031406 (2016).
14. R. A. Humphreys, L. C. Bradley, and J. Herrmann, Lincoln Lab. J. **5**, 45 (1992).
15. C. E. Max, S. S. Olivier, H. W. Friedman, J. An, K. Avicola, B. V. Beeman, H. D. Bissinger, J. M. Brase, G. V. Erbert, D. T. Gavel, K. Kanz, M. C. Liu, B. Macintosh, K. P. Neeb, J. Patience, and K. E. Waltjen, Science **277**, 1649 (1997).
16. P. Wang, S. Xie, Y. Bo, B. Wang, J. Zuo, Z. Wang, Y. Shen, F. Zhang, K. Wei, K. Jin, Y. Xu, J. Xu, Q. Peng, J. Zhang, W. Lei, D. Cui, Y. Zhang, and Z. Xu, Chin. Phys. B **23**, 094208 (2014).
17. Z. Wang, B. Zhang, J. Ning, X. Zhang, X. Su, and R. Zhao, Chin. Opt. Lett. **13**, 021403 (2015).
18. Z. H. Cong, X. Y. Zhang, Q. P. Wang, X. H. Chen, S. Z. Fan, Z. J. Liu, H. J. Zhang, X. T. Tao, J. Y. Wang, H. Y. Zhao, and S. T. Li, Laser Phys. Lett. **7**, 862 (2010).
19. M. Duering, V. Kolev, and B. Luther-Davies, Opt. Express **17**, 437 (2009).
20. J. D. Hewitt and J. G. Eden, Appl. Phys. Lett. **101**, 241109 (2012).
21. S. Hu, B. Gai, Z. Cao, J. Guo, and F. Wang, Acta Phys. Chim. Sin. **32**, 848 (2016).
22. U. Volz, M. Majerus, H. Liebel, A. Schmitt, and H. Schmoranzer, Phys. Rev. Lett. **76**, 2862 (1996).
23. G. Gautam, C. G. Parigger, D. M. Surmick, and A. M. El Sherbini, J. Quantum Spectrosc. Radiat. Transfer **170**, 189 (2016).
24. C. G. Parigger, D. M. Surmick, G. Gautam, and A. M. El Sherbini, Opt. Lett. **40**, 3436 (2015).
25. W. P. Garver, M. R. Pierce, and J. J. Leventhal, J. Chem. Phys. **77**, 1201 (1982).
26. B. P. Kibble, G. Copley, and L. Krause, Phys. Rev. **153**, 9 (1967).
27. K. C. Brown and G. O. Perram, Phys. Rev. A **85**, 022713 (2012).
28. N. D. Zameroski, G. D. Hager, W. Rudolph, and D. A. Hostutler, J. Opt. Soc. Am. B **28**, 1088 (2011).
29. N. D. Zameroski, W. Rudolph, G. D. Hager, and D. A. Hostutler, J. Phys. B: At. Mol. Opt. Phys. **42**, 245401 (2009).
30. V. N. Azyazov, S. M. Bresler, A. P. Torbin, A. M. Mebel, and M. C. Heaven, Opt. Lett. **41**, 669 (2016).
31. W. Huang, R. Tan, Z. Li, and X. Lu, Opt. Express, **23**, 31698 (2015).
32. C. B. Alcock, V. P. Itkin, and M. K. Horrigan, Can. Metall. Quart. **23**, 309 (1984).